


# Prospect and implications of $cg \rightarrow bH^+ \rightarrow bAW^+$ production at the LHC

Wei-Shu Hou<sup>1</sup> and Tanmoy Modak<sup>2</sup>

<sup>1</sup>*Department of Physics, National Taiwan University, Taipei 10617, Taiwan*

<sup>2</sup>*Institut für Theoretische Physik, Universität Heidelberg, 69120 Heidelberg, Germany*

 (Received 15 February 2021; accepted 29 March 2021; published 14 April 2021)

We study the prospect for discovering the  $cg \rightarrow bH^+ \rightarrow bAW^+$  process at the LHC. Induced by the top-flavor changing neutral Higgs coupling  $\rho_{tc}$ , the process may emerge if  $m_{H^+} > m_A + m_{W^+}$ , where  $H^+$  and  $A$  are charged and  $CP$ -odd Higgs bosons in the general two Higgs doublet model (g2HDM). We show that the  $cg \rightarrow bH^+ \rightarrow bAW^+$  process can be discovered at LHC run 3, while the full run 2 data at hand can constrain the parameter space significantly by searching for the same-sign dilepton final state. The process has unique implications on the hint of  $gg \rightarrow A \rightarrow t\bar{t}$  excess at  $m_A \approx 400$  GeV reported by CMS. When combined with other existing constraints, the  $cg \rightarrow bH^+ \rightarrow bAW^+$  process can essentially rule out the g2HDM explanation of such an excess.

DOI: [10.1103/PhysRevD.103.075015](https://doi.org/10.1103/PhysRevD.103.075015)

## I. INTRODUCTION

The discovery of the 125 GeV Higgs boson  $h$  [1] at the Large Hadron Collider (LHC) and subsequent measurements of its couplings [2] confirm that the Standard Model (SM) is the correct effective theory at the electroweak scale. While there is no compelling experimental evidence so far for new physics (NP) beyond SM, additional Higgs bosons may well exist in nature. Most ultraviolet (UV) models have extensions of the Higgs sector, while their effective descriptions at sub-TeV scale should resemble the SM. The two Higgs doublet model (2HDM) [3], with two scalar doublets  $\Phi$  and  $\Phi'$ , is one of the simplest renormalizable extensions of the SM. While the extra scalars could be at the so-called decoupling limit [4] and heavy, more interesting is when they are sub-TeV in mass, with the  $h$  boson couplings to fermions and gauge bosons SM-like as observed [5–7].

Our context would be the general two Higgs doublet model (g2HDM). Unlike the popular 2HDM-II (which automatically arises with supersymmetry), in the absence of any discrete symmetry, both the  $\Phi$  and  $\Phi'$  doublets couple to  $F = u$  and  $d$ -type quarks (as well as charged leptons). After diagonalization of the fermion mass matrices, two separate Yukawa matrices,  $\lambda_{ij}^F = \delta_{ij}\sqrt{2}m_i^F/v$  (with  $v \simeq 246$  GeV) and  $\rho_{ij}^F$ , emerge. The  $\lambda$  matrices are real and diagonal as in SM, but the  $\rho$  matrices are in general

nondiagonal and complex. It has been shown that complex  $\rho_{tt}$  [8] and  $\rho_{bb}$  [9] can each account for the observed matter-antimatter asymmetry via electroweak baryogenesis (EWBG). Our focus of interest, however, would be the flavor changing neutral Higgs (FCNH) coupling  $\rho_{tc}$ , which is found [8] to be also capable of driving EWBG [8] when  $\mathcal{O}(1)$  and with near-maximal phase.

Despite the attraction of EWBG, and the fact that we have the least knowledge about extra top Yukawa couplings, it has been raised long ago [10] the preferred absence of flavor changing neutral couplings (FCNC), such as  $\rho_{tc}$ . It is customary, therefore, to invoke a  $Z_2$  symmetry to enforce the natural flavor conservation (NFC) condition [10], that there be only one Yukawa matrix even in the 2HDM context. Caution was first raised by Cheng and Sher [11] that the NFC condition may be overkill, and, e.g.,  $\rho_{ij} \propto \sqrt{m_i m_j}/v$ , which reflects the quark mass and mixing hierarchies, could help alleviate the concerns of Ref. [10]. As the pattern implies  $\rho_{tc}$  would be the largest FCNC, thereby anticipating [12] future  $t \rightarrow ch$  or  $h \rightarrow t\bar{c}$  search, it was asserted that indeed the mass-mixing hierarchies illustrate nature’s “design,” while one does not have to adhere to the Cheng-Sher ansatz strictly.

More recently, with the SM-like  $h(125)$  lighter than the top—whereby ATLAS and CMS immediately started  $t \rightarrow ch$  (and also  $h \rightarrow \tau\mu$ ) search [13]—one notes [14] that the  $tch$  coupling should be modulated by  $\cos\gamma \equiv c_\gamma$ , the  $h-H$  mixing angle between the two  $CP$ -even Higgs bosons of 2HDM. With subsequent emergence of the “alignment” phenomenon [2], that  $h$  resembles the SM Higgs boson so well, a further nonflavor mechanism was added to nature’s design for hiding the effects of tree level FCNC’s arising from the Higgs sector: small  $c_\gamma$ . Indeed, one may not need the *ad hoc* NFC condition.

Published by the American Physical Society under the terms of the [Creative Commons Attribution 4.0 International license](https://creativecommons.org/licenses/by/4.0/). Further distribution of this work must maintain attribution to the author(s) and the published article’s title, journal citation, and DOI. Funded by SCOAP<sup>3</sup>.

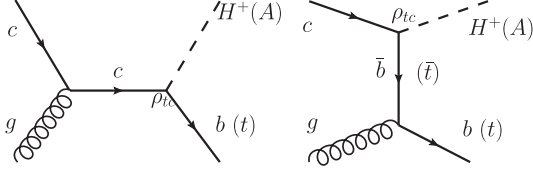


FIG. 1. Representative diagrams for  $\rho_{tc}$  induced  $cg \rightarrow bH^+$  ( $tA$ ) process.

The FCNH coupling  $\rho_{tc}$  can be discovered at the LHC via the  $cg \rightarrow tA/tH \rightarrow tt\bar{c}$  process, i.e., the same-sign top signature [15,16] (see also Refs. [17,18]). With both top quarks decaying semileptonically, the  $cg \rightarrow tA/tH \rightarrow tt\bar{c}$  process provides a clean discovery mode for  $\rho_{tc}$ , even for  $c_\gamma = 0$ . For moderate  $c_\gamma$  values, one may also have the  $cg \rightarrow bH^+ \rightarrow bhW^+$  process, which provides another sensitive probe for  $\rho_{tc}$  [19] (see also Ref. [20]).

In this article we study the prospect of probing  $\rho_{tc}$  via the novel  $cg \rightarrow bH^+ \rightarrow bAW^+$  process (conjugate process implied). The production of  $cg \rightarrow bH^+$  [21,22] is initiated by the  $\rho_{tc}$  coupling (see Fig. 1), while  $H^+ \rightarrow AW^+$  decay can occur for  $m_{H^+} > m_A + m_{W^+}$ . Like the same-sign top signature, the process also does not depend on the mixing angle  $c_\gamma$ . We study the  $cg \rightarrow bH^+ \rightarrow bAW^+$  process followed by  $\rho_{tc}$ -induced  $A \rightarrow t\bar{c}$  decay at 14 TeV LHC. With semileptonic decay of  $t$  and leptonic decay of  $W^+$ , the  $cg \rightarrow bH^+ \rightarrow bAW^+$  process could provide complementary probe for  $\rho_{tc}$ , and therefore shed light on the  $\rho_{tc}$ -driven EWBG mechanism.

We analyze also the impact of the  $cg \rightarrow bH^+ \rightarrow bAW^+$  process on the CMS hint for  $gg \rightarrow A \rightarrow t\bar{t}$  excess [23] at  $m_{t\bar{t}} \sim 400$  GeV. The ‘‘excess’’ can be explained in g2HDM [24] if  $\rho_{tt} \approx 1.1$  and  $\rho_{tc} \approx 0.9$  with  $m_H(m_{H^+}) \gtrsim 500(530)$  GeV. But this parameter range would induce also the  $cg \rightarrow bH^+ \rightarrow bAW^+$  process, which we show that it would contribute abundantly to some control region of an existing CMS search [25], hence can essentially exclude the g2HDM explanation of such an excess.

This paper is organized as follows. In Sec. II we discuss the framework and available parameter space. In Sec. III we study the prospect for the  $cg \rightarrow bH^+ \rightarrow bAW^+$  process at the LHC. Section IV is dedicated to the impact of  $cg \rightarrow bH^+ \rightarrow bAW^+$  on interpreting the CMS excess in  $gg \rightarrow A \rightarrow t\bar{t}$ . We conclude with some discussions in Sec. V.

## II. FRAMEWORK AND PARAMETER SPACE

### A. Relevant interactions

The most general  $CP$ -conserving two Higgs doublet potential can be written as [26,27]

$$V(\Phi, \Phi') = \mu_{11}^2 |\Phi|^2 + \mu_{22}^2 |\Phi'|^2 - (\mu_{12}^2 \Phi^\dagger \Phi' + \text{H.c.}) \\ + \frac{\eta_1}{2} |\Phi|^4 + \frac{\eta_2}{2} |\Phi'|^4 + \eta_3 |\Phi|^2 |\Phi'|^2 + \eta_4 |\Phi^\dagger \Phi'|^2 \\ + \left[ \frac{\eta_5}{2} (\Phi^\dagger \Phi')^2 + (\eta_6 |\Phi|^2 + \eta_7 |\Phi'|^2) \Phi^\dagger \Phi' + \text{H.c.} \right], \quad (1)$$

in the Higgs basis, where the  $\eta_i$ 's are the quartic couplings and we follow the notation of Ref. [27]. The vacuum expectation value  $v$  arises from the doublet  $\Phi$  via the minimization condition  $\mu_{11}^2 = -\frac{1}{2}\eta_1 v^2$ , while  $\langle \Phi' \rangle = 0$  (hence  $\mu_{22}^2 > 0$ ) and the second minimization condition is  $\mu_{12}^2 = \frac{1}{2}\eta_6 v^2$ . The mixing angle  $\gamma$  diagonalizes the mass-squared matrix for  $h, H$ , and satisfies [26,27]

$$c_\gamma^2 = \frac{\eta_1 v^2 - m_h^2}{m_H^2 - m_h^2}, \quad \sin 2\gamma = \frac{2\eta_6 v^2}{m_H^2 - m_h^2}. \quad (2)$$

In the alignment limit of  $c_\gamma \rightarrow 0$ ,  $h$  approaches the SM Higgs boson. The scalar masses can be expressed in terms of the parameters in Eq. (1),

$$m_{h,H}^2 = \frac{1}{2} \left[ m_A^2 + (\eta_1 + \eta_5) v^2 \mp \sqrt{(m_A^2 + (\eta_5 - \eta_1) v^2)^2 + 4\eta_6^2 v^4} \right], \quad (3)$$

$$m_A^2 = \frac{1}{2} (\eta_3 + \eta_4 - \eta_5) v^2 + \mu_{22}^2, \quad (4)$$

$$m_{H^+}^2 = \frac{1}{2} \eta_3 v^2 + \mu_{22}^2. \quad (5)$$

The scalar bosons  $h, H, A$ , and  $H^+$  in g2HDM couple to fermions by [26,28]

$$\mathcal{L} = -\frac{1}{\sqrt{2}} \sum_{F=U,D,L} \bar{F}_i [(-\lambda_{ij}^F s_\gamma + \rho_{ij}^F c_\gamma) h \\ + (\lambda_{ij}^F c_\gamma + \rho_{ij}^F s_\gamma) H - i \text{sgn}(Q_F) \rho_{ij}^F A] P_R F_j \\ - \bar{U}_i [(V \rho^D)_{ij} P_R - (\rho^{U\dagger})_{ij} P_L] D_j H^+ \\ - \bar{\nu}_i \rho_{ij}^L P_R L_j H^+ + \text{H.c.}, \quad (6)$$

where  $P_{L,R} \equiv (1 \mp \gamma_5)/2$ ,  $i, j = 1, 2, 3$  are generation indices,  $V$  is the Cabibbo-Kobayashi-Maskawa (CKM) matrix, whereas in flavor space, the  $U, D$ , and  $L$  matrices are defined as  $U = (u, c, t)$ ,  $D = (d, s, b)$ ,  $L = (e, \mu, \tau)$ , and  $\nu = (\nu_e, \nu_\mu, \nu_\tau)$ . The matrices  $\lambda_{ij}^F (\equiv \delta_{ij} \sqrt{2} m_i^F / v)$  are diagonal and real, while  $\rho_{ij}^F$  are, in general, complex and nondiagonal. In what follows we shall drop the superscript  $F$  for simplicity.

We are interested in  $cg \rightarrow bH^+ \rightarrow bAW^+$ , where  $\rho_{tc}$  induces  $cg \rightarrow bH^+$  production (Fig. 1), as one can see from Eq. (6). Unlike  $Z_2$  symmetric cases such as 2HDM type-II, intriguingly the production in g2HDM is CKM enhanced,  $V_{tb}\rho_{tc}$  [22]. There exist several direct and indirect constraints on  $\rho_{tc}$  which we shall return shortly. The decay  $H^+ \rightarrow AW^+$  on the other hand arises through

$$-\frac{g_2}{2}(A\partial^\mu H^+ - H^+\partial^\mu A)W_\mu^- + \text{H.c.}, \quad (7)$$

where  $g_2$  is SU(2) gauge coupling. Note that the  $cg \rightarrow bH^+ \rightarrow bAW^+$  process is independent of the mixing angle  $c_\gamma$ , while we consider  $A \rightarrow t\bar{c} \rightarrow bW^+\bar{c}$  final state, with both  $W^+$  bosons decaying leptonically.

### B. Constraints on parameter space

There exist several direct and indirect constraints on  $\rho_{tc}$ . For  $c_\gamma \neq 0$ ,  $\rho_{tc}$  is constrained by  $t \rightarrow ch$  search, i.e., the bounds on  $\mathcal{B}(t \rightarrow ch)$ . We take

$$\mathcal{B}(t \rightarrow ch) \approx \frac{c_\gamma^2 |\rho_{tc}|^2}{7.66 + c_\gamma^2 |\rho_{tc}|^2}, \quad (8)$$

where we approximate the total width of  $t$  quark as the sum of  $t \rightarrow bW^+$  and  $t \rightarrow ch$  partial widths. Both ATLAS and CMS have searched for the  $t \rightarrow ch$  decay and set 95% C.L. upper limits on the branching fraction. The latest ATLAS limit is  $\mathcal{B}(t \rightarrow ch) < 1.1 \times 10^{-3}$ , based on  $36.1 \text{ fb}^{-1}$  data [29] at 13 TeV, while the CMS limit of  $\mathcal{B}(t \rightarrow ch) < 4.7 \times 10^{-3}$ , based on similar dataset [30], is weaker. We find that  $|\rho_{tc}| \gtrsim 0.3$  is excluded at 95% C.L. for  $c_\gamma \sim 0.3$ . The limit weakens for smaller  $c_\gamma$  and vanishes in the alignment limit.

There are also constraints from flavor physics. For example,  $\rho_{tc}$  enters through loops with charm quarks and a charged Higgs into  $B_s - \bar{B}_s$  mixing and  $\mathcal{B}(B \rightarrow X_s \gamma)$  [31]. Reinterpreting the limits from Ref. [32], we find that  $|\rho_{tc}| \gtrsim 0.9(1.2)$  is excluded for  $m_{H^+} = 300(500)$  GeV. For the ballpark  $m_{H^+}$  values we shall consider, the flavor constraint is rather weak.

The most stringent limit on  $\rho_{tc}$  turns out to be the CMS search for four-top production [25], and comes from the control region for  $t\bar{t}W$  background, called CRW. With the signature of a same-sign dilepton pair, two  $b$ -tagged jets and  $E_T^{\text{miss}}$ , the  $cg \rightarrow bH^+ \rightarrow bAW^+ \rightarrow bt\bar{c}W^+ \rightarrow bb\bar{c}W^+W^+$  process would contribute to CRW abundantly. This is similar to the four-top constraint placed on the  $cg \rightarrow tA/tH \rightarrow t\bar{t}\bar{c}$  processes [16,24], which have identical final state topologies if both of the same-sign top quarks decay semileptonically. We shall therefore give a detailed collider study in Sec. III.

At this point we also remark that the process  $cg \rightarrow bH^+ \rightarrow bAW^+$  can also be induced by  $\rho_{ct}$  for which a similar search strategy can be adopted. In what follows we

set all  $\rho_{ij} = 0$  except  $\rho_{tc}$  for simplicity, with the impact of other  $\rho_{ij}$ 's discussed later in the paper. Furthermore, as the  $cg \rightarrow bH^+ \rightarrow bAW^+$  does not depend on  $c_\gamma$ , we simply assume the alignment limit and set  $c_\gamma = 0$  throughout the paper.

The  $cg \rightarrow bH^+ \rightarrow bAW^+$  process requires  $m_{H^+} > m_A + m_{W^+}$ . Before exploring this mass spectrum, one needs to ensure the dynamical parameters in Eq. (1) satisfy perturbativity, tree-level unitarity, and vacuum stability conditions, for which we use the public tool 2HDMC [33]. We express the quartic couplings  $\eta_1, \eta_{3-6}$  in terms of  $m_h^2, m_H^2, m_{H^+}^2, m_A, \mu_{22}^2, \gamma$ , and  $v$  [26], i.e.,

$$\eta_1 = \frac{m_h^2 s_\gamma^2 + m_H^2 c_\gamma^2}{v^2}, \quad (9)$$

$$\eta_3 = \frac{2(m_{H^+}^2 - \mu_{22}^2)}{v^2}, \quad (10)$$

$$\eta_4 = \frac{m_h^2 c_\gamma^2 + m_H^2 s_\gamma^2 - 2m_{H^+}^2 + m_A^2}{v^2}, \quad (11)$$

$$\eta_5 = \frac{m_H^2 s_\gamma^2 + m_h^2 c_\gamma^2 - m_A^2}{v^2}, \quad (12)$$

$$\eta_6 = \frac{(m_h^2 - m_H^2)(-s_\gamma)c_\gamma}{v^2}. \quad (13)$$

The quartic couplings  $\eta_2$  and  $\eta_7$  do not enter scalar masses. Imposing  $m_{H^+} > m_A + m_{W^+}$ , we randomly generate the phenomenological parameters  $\gamma, m_A, m_H, m_{H^+}, \mu_{22}, \eta_2, \eta_7$  in the following ranges:  $\mu_{22} \in [0, 1000]$  GeV,  $m_{H^+} \in [300, 600]$  GeV,  $m_A \in [200, 600 - m_{W^+}]$  GeV,  $m_H = m_{H^+}$ ,  $\eta_2 \in [0, 5]$ ,  $\eta_7 \in [-5, 5]$ , with  $m_h = 125$  GeV and  $c_\gamma = 0$  held fixed.

The randomly generated parameters are fed into 2HDMC [33] for scanning. 2HDMC uses  $\Lambda_{1-7}$  and  $m_{H^+}$  as input parameters in the Higgs basis with  $v \simeq 246$  GeV. We identify  $\eta_{1-7}$  as  $\Lambda_{1-7}$  and take  $-\pi/2 \leq \gamma \leq \pi/2$ .

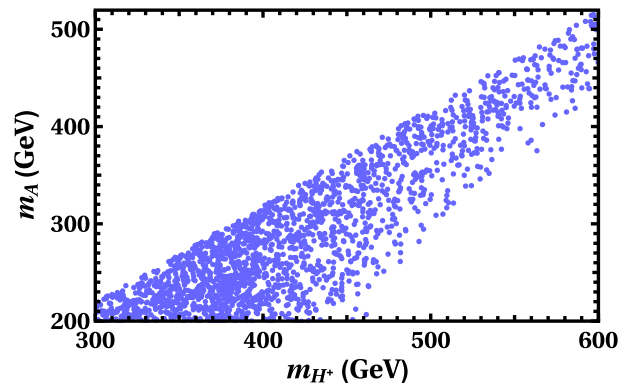


FIG. 2. Scan points satisfying  $m_{H^+} > m_A + M_{W^+}$  and consistency conditions in the  $m_{H^+} - m_A$  plane. See text for details.

TABLE I. Parameter values for the two benchmark points chosen from the scan points in Fig. 2.

BP	$\eta_1$	$\eta_2$	$\eta_3$	$\eta_4$	$\eta_5$	$\eta_6$	$\eta_7$	$m_{H^+}$ (GeV)	$m_A$ (GeV)	$m_H$ (GeV)	$\frac{\mu_{22}^2}{v^2}$
<i>a</i>	0.258	2.79	2.279	-1.342	1.342	0	-1.671	354	210	354	0.93
<i>b</i>	0.258	2.31	3.966	-2.061	2.061	0	-1.171	531	396	531	2.67

For positivity of the Higgs potential, Eq. (1), one requires  $\eta_2 > 0$ , along with other more involved conditions implemented in 2HDMC. We further conservatively demand  $|\eta_i| \leq 5$ . These scan points are plotted in the  $m_{H^+}-m_A$  plane in Fig. 2.

One also needs to consider constraints from electroweak precision [34] observables, which further restricts the hierarchical structures between the scalar masses  $m_H$ ,  $m_A$ , and  $m_{H^+}$  [35,36], and therefore  $\eta_i$ s. For the sake of simplicity, we have taken  $m_H = m_{H^+}$ , which corresponds to twisted custodial symmetry [37]. In general, for non-degenerate  $m_H$  and  $m_{H^+}$ , the randomly generated parameters that passed unitarity, perturbativity, and positivity conditions from 2HDMC, can easily be tested for the oblique parameter constraints [38] also in 2HDMC.<sup>1</sup>

It is clear from Fig. 2 that there exist a significant range of scan points that can facilitate  $H^+ \rightarrow AW^+$  decay. We choose two benchmark points (BPs) from Fig. 2 for illustration, and list the parameter values in Table I.

### III. PROSPECT AT THE LHC

We now discuss the constraint from the CRW region of the CMS  $4t$  search on  $\rho_{tc}$ , and illustrate with our BPs.

#### A. Constraints from CMS $4t$ -CRW

The CMS search for SM  $4t$  production [25] is based on  $137 \text{ fb}^{-1}$  data at  $\sqrt{s} = 13 \text{ TeV}$ , i.e., with full run 2 data. Based on the number of  $b$ -tagged jets and charged leptons ( $e, \mu$ ), the CMS search divides its analysis into several signal regions (SRs) and two control regions (CRs). The baseline selection criterion requires each event should have at least two same-sign leptons. The remaining selection cuts goes as follows [25]: The leading and subleading leptons should have  $p_T > 25$  and  $20 \text{ GeV}$ , respectively, with electron (muon) pseudorapidity satisfying  $|\eta| < 2.5$  (2.4), whereas all jets should satisfy  $|\eta| < 2.4$ . Events are selected if  $p_T$  of the jets and  $b$  jets fulfill any of the following three criteria [42]: (i) both  $b$  jets satisfy  $p_T > 40 \text{ GeV}$ ; (ii) one  $b$  jet with  $p_T > 20 \text{ GeV}$  and  $20 < p_T < 40 \text{ GeV}$  for the second  $b$  jet, but  $p_T > 40 \text{ GeV}$  for the third jet; (iii) both  $b$  jets should satisfy  $20 < p_T < 40 \text{ GeV}$ , but with two extra jets each with  $p_T > 40 \text{ GeV}$ . Defining  $H_T$  as the scalar sum of the  $p_T$  of all jets [25], CMS requires  $H_T > 300$  and  $p_T^{\text{miss}} > 50 \text{ GeV}$ .

<sup>1</sup>Further details on parameter counting and the scanning procedure can be found in Refs. [28,39–41].

To reduce the charge-misidentified Drell-Yan ( $Z/\gamma^*$ ) background with electrons, events with same-sign electron pairs with  $m_{ee} < 12 \text{ GeV}$  are rejected. With these selection criteria, the expected total number of events (SM backgrounds plus  $4t$ ) in the CRW are  $335 \pm 18$ , with 338 events observed [25].

It is found [16,24,43,44] that the most stringent constraint on  $\rho_{tc}$  arises from the CRW, or  $t\bar{t}W$  control region [25]. These works studied the  $\rho_{tc}$ -induced  $cg \rightarrow tH/tA \rightarrow t\bar{t}\bar{c}$  processes. When both the same-sign top quarks decay semileptonically, these processes would contribute to the CRW. But the  $cg \rightarrow bH^+ \rightarrow bAW^+$  process with  $A \rightarrow t\bar{c}$  would also contribute to the CRW if the top decays semileptonically and the  $W^+$  decays leptonically. To estimate the CRW constraints for our BPs, one has to add contributions from both  $cg \rightarrow bH^+ \rightarrow bAW^+$  and  $cg \rightarrow tH/tA \rightarrow t\bar{t}\bar{c}$  coherently, as both effectively give  $cg \rightarrow \ell^+ \ell^+ bb\nu_{\ell}\nu_{\ell}\bar{c}$ , which we denote as the same-sign dilepton with  $2b$  plus extra jet ( $SS2l - 2bj$ ) signature. Because of multiple contributing processes that are added at the amplitude level, one cannot obtain simple  $\sigma \times \mathcal{B}$  scaling formulas for the BPs. Therefore, unlike mass vs  $\rho_{tc}$  exclusion contours as in Refs. [16,43,44], here we test directly whether a reference  $\rho_{tc}$  value survives the CRW constraint. In particular, we take the relatively low  $\rho_{tc} = 0.15$  for illustration.

Under the aforementioned assumptions on couplings, i.e., turning off all other  $\rho_{ij}$  except  $\rho_{tc}$ , the total decay width of  $H^+$  is the sum of  $H^+ \rightarrow c\bar{b}$  and  $H^+ \rightarrow AW^+$  partial widths, while for  $H$  it is the combination of  $H \rightarrow t\bar{c} + \bar{t}c$  and  $H \rightarrow AZ$  decays for both the BPs, with  $\mathcal{B}(A \rightarrow t\bar{c} + \bar{t}c) = 100\%$ . For  $\rho_{tc} = 0.15$ , the total decay widths of  $A$ ,  $H$  and  $H^+$  are  $2.04$  (2.27),  $0.029$  (0.35), and  $2.65$  (2.9)  $\text{GeV}$  for BP*a* (BP*b*).

We first generate  $SS2l - 2bj$  events for both the BPs at  $\sqrt{s} = 13 \text{ TeV}$  using MadGraph5\_aMC@NLO [45] (denoted as MadGraph5\_aMC) at leading order (LO) with default parton distribution function (PDF) set NN23LO1 [46], and interface with PYTHIA 6.4 [47] for showering and hadronization. The events are then fed into DELPHES 3.4.2 [48] for fast detector simulation. Here in our exploratory analysis we use the default CMS-based detector card of DELPHES 3.4.2 for the CMS CRW to incorporate detector effects such as  $b$  tagging and light-jet misidentification efficiencies, etc. The jets are reconstructed via anti- $k_T$  algorithm with radius parameter  $R = 0.5$ . The effective model is implemented in the FeynRules [49] framework.

Following the same event selection cuts of the CRW, the  $SS2l - 2bj$  cross section for the two BPs are 0.283 and 0.245 fb. Multiplying by the  $137 \text{ fb}^{-1}$  integrated luminosity, these translate to  $\sim 39$  and 34 events, respectively, which should have shown up already in the CRW of CMS  $4t$  search [25]. Demanding that the combination of the number of events expected from the SM and the  $\rho_{tc}$ -induced same-sign dilepton with  $2b$  plus extra jet events agree with the observed number of events within  $2\sigma$  uncertainty of the expected, we see that  $\rho_{tc} = 0.15$  is barely allowed for either BPs. We note that  $\rho_{tc} \gtrsim 0.15$  is the ballpark exclusion limit found in Ref. [44] from  $SS2l - 2bj$  arising from  $cg \rightarrow tH/tA \rightarrow t\bar{t}c$  processes alone, with a mass hierarchy  $m_H \sim m_A \sim m_{H^+}$ , but the  $cg \rightarrow bH^+ \rightarrow bAW^+$  process was not induced. This illustrates that  $SS2l - 2bj$  events arising from  $cg \rightarrow bH^+ \rightarrow bAW^+$  is significant, and CRW constrains  $\rho_{tc}$  more stringently if  $m_{H^+} > m_A + m_{W^+}$ . Here we remark that the constraint from CRW is extracted with default CMS based detector card of DELPHES. In our exploratory analysis, we have not validated the results of Ref. [25] which we leave out for future. In any case, we would see shortly that a dedicated  $SS2l - 2bj$  search could be more sensitive than the constraint from CRW.

ATLAS has also made similar search [50] but due to difference in defining SRs and selection criteria, the constraints [43] are found to be weaker than CMS. Other searches such as for squark pair production [51], and for new phenomena with same-sign dileptons and  $b$  jets [52], both by ATLAS, have too strong selection cuts to give meaningful constraint.

### B. A dedicated $SS2l - 2bj$ search

Even though the existing CMS  $4t$  search with full run 2 data can set meaningful constraints on the parameter space, it is not optimized for  $cg \rightarrow bH^+ \rightarrow bAW^+$  search. This motivates us to perform a dedicated search for  $SS2l - 2bj$  for our BPs at 14 TeV LHC. Here, we closely follow the analysis of Ref. [44].

There are several SM backgrounds for a dedicated  $SS2l - 2bj$  search. The dominant ones are  $t\bar{t}Z$ ,  $t\bar{t}W$ , with  $4t$ ,  $t\bar{t}h$  and  $tZ$ + jets subdominant. In addition, if the lepton charge gets misidentified (charge or  $Q$  flip), with misidentification efficiency at  $2.2 \times 10^{-4}$  [52–54], the  $t\bar{t}$ + jets and  $Z/\gamma^*$ + jets processes would also contribute. We remark that the CMS study [55] with similar final state topology but with slightly different cuts finds “nonprompt” backgrounds at  $\sim 1.5$  times the  $t\bar{t}W$  background, which is significant. As the nonprompt backgrounds are not properly modeled in Monte Carlo simulations, we simply add this component to the overall background at 1.5 times the  $t\bar{t}W$  background after selection cuts. There are also some tiny backgrounds such as  $3t + W$  and  $3t + j$ , which we neglect in our analysis.

For generating signal and background event samples, we follow the procedure as in the previous section and adopt MLM matching [56,57] prescription for a matrix element and parton shower merging. We allow one additional parton for  $t\bar{t}Z$ ,  $t\bar{t}W$ , and  $t\bar{t}$ + jets, while for other backgrounds and the signal we do not consider additional partons. This restriction is due to computational limitations in this first attempt, and we adopt a default ATLAS based detector card of DELPHES 3.4.2.

The LO cross sections of  $t\bar{t}Z$ ,  $t\bar{t}W^-$  ( $t\bar{t}W^+$ ),  $4t$ ,  $t\bar{t}h$ , and  $tZ$ + jets are normalized to next-to-leading order (NLO) by the factors 1.56 [58], 1.35 (1.27) [59], 2.04 [45], 1.27 [60] and 1.44 [45], respectively. The same QCD correction factor is taken for the charge conjugate  $t\bar{t}Z$ + jets background for simplicity. The  $Q$ -flip  $t\bar{t}$ + jets and  $Z/\gamma^*$ + jets components are adjusted to NNLO cross sections by factors of 1.84 [61] and 1.27, respectively, where we use FEWZ 3.1 [62] to obtain the latter.

To reduce backgrounds, we follow a cut based analysis that differs from the CRW of Ref. [25]. The leading and subleading leptons are required to have  $p_T > 25$  and 20 GeV, respectively, while  $|\eta| < 2.5$  for both leptons. All three jets should have  $p_T > 20$  GeV, whereas  $|\eta| < 2.5$ . The  $E_T^{\text{miss}}$  in each event should be  $> 35$  GeV. The  $\Delta R$  separation between any lepton and any jets ( $\Delta R_{\ell j}$ ), between the two  $b$  jets ( $\Delta R_{bb}$ ), and between the same-sign leptons ( $\Delta R_{\ell\ell}$ ), should all satisfy  $\Delta R > 0.4$ . Finally, all selected events should have  $H_T > 300$  GeV, with  $H_T$  defined according to ATLAS, i.e., including the  $p_T$  of the two leading same-sign leptons.

The background cross sections after selection cuts are summarized in Table II, while the signal cross sections along with significance for the corresponding BPs are given in Table III. The significance is computed using the likelihood for a simple counting experiment [63],

$$Z(n|n_{\text{pred}}) = \sqrt{-2 \ln \frac{L(n|n_{\text{pred}})}{L(n|n)}}, \quad (14)$$

with  $L(n|\bar{n}) = e^{-\bar{n}} \bar{n}^n / n!$ , where  $n$  ( $n_{\text{pred}}$ ) is the observed (predicted) number of events. For discovery, one compares the signal plus background ( $s + b$ ) with the background

TABLE II. Background cross sections after selection cuts for the dedicated  $SS2l - 2bj$  search.

Backgrounds	Cross section (fb)
$t\bar{t}W$	1.31
$t\bar{t}Z$	1.97
$4t$	0.316
$tZ$ + jets	0.255
$t\bar{t}h$	0.07
$Q$ flip	0.024
nonprompt	$1.5 \times t\bar{t}W$

TABLE III. Signal cross sections and significances with 300(3000) fb<sup>-1</sup> for the BPs of SS2l – 2bj search after selection cuts.

BP	Signal (fb)	Significance ( $\mathcal{Z}$ ) 300(3000) fb <sup>-1</sup>
<i>a</i>	0.468	3.3 (10.4)
<i>b</i>	0.334	2.4 (7.5)

prediction (*b*) and demand  $Z(s + b|b) > 5$ , while for exclusion we demand  $Z(b|s + b) > 2$ .

We see from Table III that, for BP*a* one can reach the significance of  $\sim 3.3\sigma(10.4\sigma)$  with 300(3000) fb<sup>-1</sup>, while correspondingly  $\sim 2.4\sigma(7.5\sigma)$  for BP*b*. Reanalyzing for a reference value of  $\rho_{tc} = 0.1$ , we find that significances at  $\sim 2.8\sigma(4.8\sigma)$ ,  $\sim 2\sigma(3.5\sigma)$  are possible for BP*a*, BP*b* with 1000(3000) fb<sup>-1</sup>. For exclusion, we find that  $\rho_{tc} = 0.1$  can be excluded for BP*a* (BP*b*) with 600(1000) fb<sup>-1</sup> data. Thanks to the presence of the  $cg \rightarrow bH^+ \rightarrow bAW^+$  process, these are *well below* the exclusion reach of HL-LHC data based on the  $cg \rightarrow tA/tH \rightarrow tt\bar{c}$  process alone, as was found in Ref. [44].

#### IV. IMPACT ON THE CMS EXCESS

In studying the prospect of  $cg \rightarrow bH^+ \rightarrow bAW^+ \rightarrow b\bar{t}cW^+ \rightarrow W^+W^+bb\bar{c}$  at the LHC, because of interference with the  $cg \rightarrow tH/A \rightarrow tt\bar{c}$  in the same final state, we find elevated impact. Given the correlation [24] of the  $cg \rightarrow tH/A \rightarrow tt\bar{c}$  process and the  $gg \rightarrow A \rightarrow t\bar{t}$  excess hinted by CMS [23], the  $cg \rightarrow bH^+ \rightarrow bAW^+$  process should therefore make strong impact on the g2HDM interpretation, which we now turn to elucidate.

CMS has reported [23] a hint of excess in  $gg \rightarrow H/A \rightarrow t\bar{t}$  resonance search with 35.9 fb<sup>-1</sup> data at 13 TeV. The search fits for a peak and dip structure [64] in the  $t\bar{t}$  invariant mass ( $m_{t\bar{t}}$ ) from interference between  $gg \rightarrow H/A \rightarrow t\bar{t}$  and the rather large  $gg \rightarrow t\bar{t}$  QCD background. A signal-like deviation is reported [23] around  $m_A = 400$  GeV and  $\Gamma_A/m_A = 4\%$  from a model-independent analysis. The local significance is  $(3.5 \pm 0.3)\sigma$ , becoming  $1.9\sigma$  if one takes into account look-elsewhere effect. The deviation depends mildly on  $\Gamma_A/m_A$ , while no deviation is seen for the *CP*-even scalar boson *H*. CMS does not provide the  $A\bar{t}\bar{t}$  coupling strength, using instead a ‘‘coupling modifier’’  $g_{A\bar{t}\bar{t}}$  [23], which is nothing but  $g_{A\bar{t}\bar{t}} = \rho_{tt}/\lambda_t$  in g2HDM, and one can utilize the Supplemental Material of Ref. [23] to infer its value. Note that ATLAS [65] has performed a similar search for distorted Breit-Wigner shape in  $m_{t\bar{t}}$  with 8 TeV data for  $m_{A,H} > 500$  GeV, with no excess seen.

The CMS excess is rather close to the  $t\bar{t}$  threshold, and one needs a better understanding of the interference with signal near threshold, and even  $gg \rightarrow t\bar{t}$  production in SM as well. Nevertheless, it is of interest to see whether the

excess can be interpreted in g2HDM. Taking  $g_{A\bar{t}\bar{t}} = 1.1$  (hence  $\rho_{tt} \approx 1.1$ ), Ref. [24] treated the 95% C.L. upper limit at  $m_A = 400$  GeV with  $\Gamma_A/m_A = 5\%$  as the closest (among the six plots given in Ref. [23]) to the reported  $3.5\sigma$  excess with  $\Gamma_A/m_A = 4\%$ , but it would have been preferable to have CMS provide the coupling modifier value for the excess. It was found [24] that the excess at  $m_A = 400$  GeV with  $\rho_{tt} \sim 1.1$  can be compatible with  $\rho_{tc} \sim 0.9$  and  $m_H \gtrsim 500$  GeV,  $m_{H^+} \gtrsim 530$  GeV in g2HDM. This took into account various constraints similar to those considered in Sec. II B, plus  $pp \rightarrow \bar{t}(b)H^+ \rightarrow \bar{t}(b)t\bar{b}$  searches, and also neutral Higgs searches such as  $pp \rightarrow t\bar{t}A/\bar{t}\bar{t}H \rightarrow t\bar{t}\bar{t}$  [25], as well as the limits from  $gg \rightarrow H \rightarrow t\bar{t}$  searches by CMS [23] and ATLAS [65]. These need to be retraced with adding the amplitude induced by  $cg \rightarrow bH^+ \rightarrow bAW^+$ .

But before that, we remark that the sizable  $\rho_{tc} \sim 0.9$  value plays a mutually compensating role with the large  $\rho_{tt} \sim 1.1$  needed to account for the CMS excess. Sizable  $\rho_{tc}$  dilutes  $\mathcal{B}(A/H \rightarrow t\bar{t})$  ( $\mathcal{B}(H^+ \rightarrow t\bar{b})$ ) by  $A/H \rightarrow t\bar{c} + \bar{t}c$  ( $H^+ \rightarrow c\bar{b}$ ) decays, hence weakens the constraints from  $pp \rightarrow t\bar{t}A/\bar{t}\bar{t}H \rightarrow t\bar{t}\bar{t}$  and  $gg \rightarrow H \rightarrow t\bar{t}$  ( $pp \rightarrow \bar{t}(b)H^+ \rightarrow \bar{t}(b)t\bar{b}$ ) searches. In turn,  $\rho_{tt} \sim 1.1$  helps alleviate the constraint on  $\rho_{tc}$  from  $cg \rightarrow tA/tH \rightarrow tt\bar{c}$  by finite  $\mathcal{B}(A/H \rightarrow t\bar{t})$ . The most stringent constraint arises from SR12 of CMS [25] search, the signal region (SR) for SM  $4t$  production, defined as at least three charged leptons ( $e, \mu$ ), three *b*-tagged jets but restricting to four jets, plus some  $E_T^{\text{miss}}$ . CMS observed 2 events in SR12 in the cut-based analysis whereas  $2.62 \pm 0.54$  events were expected [25]. With both  $\rho_{tt} \sim 1.1$  and  $\rho_{tc} \sim 0.9$ , the  $cg \rightarrow tA/tH \rightarrow tt\bar{t}$  process would contribute to SR12 if all three top decays semileptonically, but it was found to be compatible with SR12 [24].

Most constraints analyzed in Ref. [24] remain the same, but new LHC results on  $pp \rightarrow \bar{t}(b)H^+ \rightarrow \bar{t}(b)t\bar{b}$  search became available [66,67] and seem to push  $m_{H^+}$  toward the heavier side, making the benchmark point analyzed in Ref. [24] incompatible with the excess. We find a new allowed benchmark point, summarized in Table IV, that can account for the excess while satisfying perturbativity, unitarity, positivity, and electroweak precision measurements (checked via 2HDMC [33]), as well as all experimental constraints described in Ref. [24], while taking into account the new results from Refs. [66,67]. The total widths of *A*, *H* and *H*<sup>+</sup> for this BP are  $\sim 30, 87$ , and 105 GeV, respectively. The respective branching ratios are  $A \rightarrow t\bar{t}$  and  $t\bar{c} + \bar{t}c \approx 48\%$  and  $52\%$ ;  $H \rightarrow t\bar{t}$ ,  $t\bar{c} + \bar{t}c$  and  $AZ \approx 35\%$ ,  $40\%$  and  $25\%$ ; and  $H^+ \rightarrow t\bar{b}$ ,  $c\bar{b}$  and  $AW^+ \approx 40\%$ ,  $38\%$  and  $22\%$ . We neglect tiny loop induced decays for simplicity.

The spectrum in Table IV would again allow the  $cg \rightarrow bH^+ \rightarrow bAW^+$  process, and therefore contribute to the CRW of Ref. [25]. We generate SS2l – 2bj events from  $cg \rightarrow bH^+ \rightarrow bAW^+$  and  $cg \rightarrow tA/tH \rightarrow tt\bar{c}$  at

TABLE IV. Parameter values to interpret the  $gg \rightarrow A \rightarrow t\bar{t}$  excess hinted by CMS [23].

$\rho_{tt}$	$\rho_{tc}$	$\eta_1$	$\eta_2$	$\eta_3$	$\eta_4$	$\eta_5$	$\eta_6$	$\eta_7$	$m_{H^+}$ (GeV)	$m_A$ (GeV)	$m_H$ (GeV)	$\frac{\mu_{22}^2}{v^2}$
1.1	1	0.258	1.894	8.872	-4.772	4.752	0	-0.514	670	400	670	2.96

$\sqrt{s} = 13$  TeV for this BP. Following the same selection criteria and procedure as described in Sec. III A, we find the  $SS2l - 2bj$  cross section to be  $\sim 1.3$  fb. Multiplying by  $137 \text{ fb}^{-1}$  integrated luminosity, this translates to an overwhelming 179 events. This suggests that the BP and hence the g2HDM interpretation of the CMS excess is already in severe tension with the CRW of Ref. [25]. At this point we also remark that the BP in Table IV has twisted custodial symmetry i.e.,  $m_{H^+} = m_H$ , which helped us evade stringent electroweak precision observables such as  $T$  parameter. In general mass splitting between  $m_H$  and  $m_{H^+}$  is possible however, such choice would lead to stringent constraints from electroweak precision observables. In addition, for lighter  $m_H$ , in particular for  $m_{H^+} > m_H + m_{W^+}$  the  $cg \rightarrow bH^+ \rightarrow bHW^+$  process with  $H \rightarrow t\bar{c}$  decay would also induce  $SS2l - 2bj$  signature and contribute to CRW region.

The presence of other  $\rho_{ij}$ 's may reduce the required  $\rho_{tc}$  for the excess, but would be subject to other stringent constraints from flavor physics and LHC. For example,  $\rho_{tu}$  can still be sizable [43], which would also induce  $SS2l - 2bj$  events via  $V_{tb}$ -enhanced  $ug \rightarrow bH^+ \rightarrow bAW^+$  process, as well as the  $ug \rightarrow tA/tH \rightarrow t\bar{t}u$  process. Having both  $\rho_{tu}$  and  $\rho_{tc}$ , one would need to consider stringent constraints from  $D-\bar{D}$  mixing [31,32]. A nonvanishing  $\rho_{\tau\tau}$  may help reduce the requirement of large  $\rho_{tc}$ . However, together with  $\rho_{tt}$ , such parameter space would also receive several meaningful constraints from flavor physics and low energy observables (see, e.g., Refs. [21,32,68,69]). Presence of  $\rho_{bb}$  would make the situation worse via  $V_{tb}$  enhanced  $pp \rightarrow \bar{t}(b)H^+ \rightarrow \bar{t}(b)t\bar{b}$  process, in addition to other stringent constraints as discussed in Refs. [40,41]. We therefore do not think in its minimal set up g2HDM can explain the CMS hint for an excess at  $m_A \approx 400$  GeV.

## V. DISCUSSION AND OUTLOOK

We have analyzed the possibility of probing the FCNH coupling  $\rho_{tc}$  at the LHC via the  $cg \rightarrow bH^+ \rightarrow bAW^+$  process at 14 TeV LHC. With the novel signature of same-sign dilepton plus  $2b$  and an extra jet ( $SS2l - 2bj$ ), the process can be discovered even for  $\rho_{tc}$  down to 0.1.

Some uncertainties in our results have not been covered. The  $c$ -quark initiated  $cg \rightarrow bH^+$ ,  $tA/tH$  processes have non-negligible systematic uncertainties such as from PDF and scale dependence (see, e.g., Refs. [70–72]), which we did not include in our analysis. Moreover, we have not included nonprompt and fake backgrounds. These induce some uncertainties in our results.

The FCNH coupling  $\rho_{tu}$ , as mentioned, can also induce similar final state topologies via the  $ug \rightarrow bH^+ \rightarrow bAW^+$  process. One may distinguish between the  $\rho_{tc}$  and  $\rho_{tu}$  induced processes via charge asymmetry of positively and negatively charged dilepton signature, as discussed in Ref. [43]. Presence of both  $\rho_{tc}$  and  $\rho_{tu}$  can obscure the role of each other. However, in such a case,  $D-\bar{D}$  mixing can provide some probe [31,32]. For example, Ref. [31] found that  $|\rho_{tu}^*\rho_{tc}| \gtrsim 0.02$  could be excluded by  $D-\bar{D}$  mixing for  $m_H \approx m_A \approx m_{H^+} \approx 500$  GeV. Moreover, non-zero  $\rho_{tu}$ , with the help of nonzero  $\rho_{\tau\tau}$ , can induce observable effects in the branching ratio of  $B \rightarrow \mu\nu$  [73], which is within reach of Belle-II [74].

We have focused mainly on the parameter space where all other  $\rho_{ij}$ 's vanish. However, the  $\rho_{ij}$  couplings would likely share [12,27] the same flavor organization as in SM, i.e.,  $\rho_{ii} \sim \lambda_i$ , while off-diagonal elements trickle off. This would suppress the discovery potential of  $SS2l - 2bj$  signature to some extent, where we have discussed the impact of  $\mathcal{O}(1)\rho_{tt}$  in Sec. IV. Finite  $\rho_{tt}$  actually motivates conventional searches such as  $gg \rightarrow H$ ,  $A \rightarrow t\bar{t}$  and  $gg \rightarrow Ht\bar{t} \rightarrow t\bar{t}t\bar{t}$  [75]. Furthermore, if  $\rho_{tc}$  and  $\rho_{tt}$  are both finite, one may have the more exquisite  $cg \rightarrow tA/tH \rightarrow t\bar{t}$  [15] and  $cg \rightarrow bH^+ \rightarrow bt\bar{b}$  processes [22], where the latter may emerge in LHC run 3.

We find that the  $SS2l - 2bj$  signature arising from  $cg \rightarrow bH^+ \rightarrow bAW^+$  and  $cg \rightarrow tA/tH \rightarrow t\bar{t}c$  processes together can exclude a g2HDM interpretation of the  $gg \rightarrow A \rightarrow t\bar{t}$  excess hinted by CMS [25]. One may push  $H^+$  to avoid such constraint, but this should also be tightly constrained by electroweak precision measurements as well as perturbativity. The latter tension can be readily seen from the  $\eta_3$  value in Table IV. The presence of multiple nonvanishing  $\rho_{ij}$  may help alleviate the tension. However, we remark that such an effort would require a more involved analysis, which we leave for the future.

In summary, we have analyzed the prospect for discovering the  $cg \rightarrow bH^+ \rightarrow bAW^+$  process at the 14 TeV LHC, and show that it receives stringent constraint from some control region of the existing CMS  $4t$  search. We find that a dedicate search with the signature of same-sign dilepton, two  $b$ -tagged jets plus an additional jet and missing transverse energy can provide better probe of the parameter space. The process can essentially exclude the g2HDM explanation of  $gg \rightarrow A \rightarrow t\bar{t}$  excess observed by CMS. If the  $cg \rightarrow bH^+ \rightarrow bAW^+$  process is discovered, it would not only confirm the existence of new physics, it may also help us understand the mechanism behind the observed baryon asymmetry of the Universe.

## ACKNOWLEDGMENTS

The work of T. M. is supported by a postdoctoral research fellowship from the Alexander von Humboldt Foundation. The work of W. S. H. is supported by MOST 109-2112-M-002-015-MY3 of Taiwan and NTU 110L104019 and 110L892101.

- 
- [1] G. Aad *et al.* (ATLAS Collaboration), *Phys. Lett. B* **716**, 1 (2012); S. Chatrchyan *et al.* (CMS Collaboration), *ibid.* **716**, 30 (2012).
- [2] G. Aad *et al.* (ATLAS and CMS Collaborations), *J. High Energy Phys.* **08** (2016) 045; A. M. Sirunyan *et al.* (CMS Collaboration), *Eur. Phys. J. C* **79**, 421 (2019); G. Aad *et al.* (ATLAS Collaboration), *Phys. Rev. D* **101**, 012002 (2020).
- [3] For pedagogical reviews on 2HDM, see e.g. A. Djouadi, *Phys. Rep.* **457**, 1 (2008); G. C. Branco, P. M. Ferreira, L. Lavoura, M. N. Rebelo, M. Sher, and J. P. Silva, *Phys. Rep.* **516**, 1 (2012); and references therein.
- [4] J. F. Gunion and H. E. Haber, *Phys. Rev. D* **67**, 075019 (2003).
- [5] A. Biekötter, T. Corbett, and T. Plehn, *SciPost Phys.* **6**, 064 (2019).
- [6] J. Ellis, C. W. Murphy, V. Sanz, and T. You, *J. High Energy Phys.* **06** (2018) 146.
- [7] E. da Silva Almeida, A. Alves, N. Rosa Agostinho, O. J. P. Eboli, and M. C. Gonzalez-Garcia, *Phys. Rev. D* **99**, 033001 (2019).
- [8] K. Fuyuto, W.-S. Hou, and E. Senaha, *Phys. Lett. B* **776**, 402 (2018).
- [9] T. Modak and E. Senaha, *Phys. Rev. D* **99**, 115022 (2019).
- [10] S. L. Glashow and S. Weinberg, *Phys. Rev. D* **15**, 1958 (1977).
- [11] T. P. Cheng and M. Sher, *Phys. Rev. D* **35**, 3484 (1987).
- [12] W.-S. Hou, *Phys. Lett. B* **296**, 179 (1992).
- [13] P. A. Zyla *et al.* (Particle Data Group), *Prog. Theor. Exp. Phys.* **2020**, 083C01 (2020).
- [14] K.-F. Chen, W.-S. Hou, C. Kao, and M. Kohda, *Phys. Lett. B* **725**, 378 (2013).
- [15] M. Kohda, T. Modak, and W.-S. Hou, *Phys. Lett. B* **776**, 379 (2018).
- [16] W.-S. Hou, M. Kohda, and T. Modak, *Phys. Lett. B* **786**, 212 (2018).
- [17] W.-S. Hou, G.-L. Lin, C.-Y. Ma, and C.-P. Yuan, *Phys. Lett. B* **409**, 344 (1997).
- [18] Without detailed studies, the process was also discussed by Ref. [19] and W. Altmannshofer, J. Eby, S. Gori, M. Lotito, M. Martone, and D. Tuckler, *Phys. Rev. D* **94**, 115032 (2016); W. Altmannshofer, B. Maddock, and D. Tuckler, *ibid.* **100**, 015003 (2019). See also Ref. [20] where the  $pp \rightarrow t\bar{c}H$  process was discussed.
- [19] W.-S. Hou, T. Modak, and T. Plehn, [arXiv:2012.03572](https://arxiv.org/abs/2012.03572).
- [20] S. Gori, C. Grojean, A. Juste, and A. Paul, *J. High Energy Phys.* **01** (2018) 108. In this reference without detailed collider study, the authors discussed  $gg \rightarrow c\bar{b}H^+$  process followed by  $H^+ \rightarrow hW^+$  decay.
- [21] S. Iguro and K. Tobe, *Nucl. Phys.* **B925**, 560 (2017).
- [22] D. K. Ghosh, W.-S. Hou, and T. Modak, *Phys. Rev. Lett.* **125**, 221801 (2020).
- [23] A. M. Sirunyan *et al.* (CMS Collaboration), *J. High Energy Phys.* **04** (2020) 171.
- [24] W.-S. Hou, M. Kohda, and T. Modak, *Phys. Lett. B* **798**, 134953 (2019).
- [25] A. M. Sirunyan *et al.* (CMS Collaboration), *Eur. Phys. J. C* **80**, 75 (2020).
- [26] See, e.g., S. Davidson and H. E. Haber, *Phys. Rev. D* **72**, 035004 (2005).
- [27] W.-S. Hou and M. Kikuchi, *Europhys. Lett.* **123**, 11001 (2018).
- [28] W.-S. Hou and T. Modak, *Phys. Rev. D* **101**, 035007 (2020).
- [29] M. Aaboud *et al.* (ATLAS Collaboration), *J. High Energy Phys.* **05** (2019) 123.
- [30] A. M. Sirunyan *et al.* (CMS Collaboration), *J. High Energy Phys.* **06** (2018) 102.
- [31] B. Altunkaynak, W.-S. Hou, C. Kao, M. Kohda, and B. McCoy, *Phys. Lett. B* **751**, 135 (2015).
- [32] A. Crivellin, A. Kokulu, and C. Greub, *Phys. Rev. D* **87**, 094031 (2013).
- [33] D. Eriksson, J. Rathsman, and O. Stål, *Comput. Phys. Commun.* **181**, 189 (2010).
- [34] M. E. Peskin and T. Takeuchi, *Phys. Rev. D* **46**, 381 (1992).
- [35] C. D. Froggatt, R. G. Moorhouse, and I. G. Knowles, *Phys. Rev. D* **45**, 2471 (1992).
- [36] H. E. Haber and O. Stål, *Eur. Phys. J. C* **75**, 491 (2015).
- [37] J.-M. Gérard and M. Herquet, *Phys. Rev. Lett.* **98**, 251802 (2007).
- [38] M. Baak, J. Cúth, J. Haller, A. Hoecker, R. Kogler, K. Mönig, M. Schott, and J. Stelzer (Gfitter Group), *Eur. Phys. J. C* **74**, 3046 (2014). The latest values of oblique parameters are obtained from Gfitter website: [http://project-gfitter.web.cern.ch/project-gfitter/Oblique\\_Parameters/](http://project-gfitter.web.cern.ch/project-gfitter/Oblique_Parameters/).
- [39] W.-S. Hou, M. Kohda, and T. Modak, *Phys. Rev. D* **99**, 055046 (2019).
- [40] T. Modak, *Phys. Rev. D* **100**, 035018 (2019).
- [41] T. Modak and E. Senaha, *J. High Energy Phys.* **11** (2020) 025.
- [42] We thank K.-F. Chen for clarifications on this point.
- [43] W.-S. Hou, T.-H. Hsu, and T. Modak, *Phys. Rev. D* **102**, 055006 (2020).
- [44] W.-S. Hou and T. Modak, *Mod. Phys. Lett. A* **36**, 2130006 (2021).



- [45] J. Alwall, R. Frederix, S. Frixione, V. Hirschi, F. Maltoni, O. Mattelaer, H.-S. Shao, T. Stelzer, P. Torrielli, and M. Zaro, *J. High Energy Phys.* **07** (2014) 079.
- [46] R. D. Ball, V. Bertone, S. Carrazza, L. Del Debbio, S. Forte, A. Guffanti, N. P. Hartland, and J. Rojo (NNPDF Collaboration), *Nucl. Phys.* **B877**, 290 (2013).
- [47] T. Sjöstrand, S. Mrenna, and P. Skands, *J. High Energy Phys.* **05** (2006) 026.
- [48] J. de Favereau, C. Delaere, P. Demin, A. Giammanco, V. Lemaitre, A. Mertens, and M. Selvaggi (DELPHES 3 Collaboration), *J. High Energy Phys.* **02** (2014) 057.
- [49] A. Alloul, N. D. Christensen, C. Degrande, C. Duhr, and B. Fuks, *Comput. Phys. Commun.* **185**, 2250 (2014).
- [50] G. Aad *et al.* (ATLAS Collaboration), *Eur. Phys. J. C* **80**, 1085 (2020).
- [51] G. Aad *et al.* (ATLAS Collaboration), *J. High Energy Phys.* **06** (2020) 046.
- [52] M. Aaboud *et al.* (ATLAS Collaboration), *J. High Energy Phys.* **12** (2018) 039.
- [53] The ATLAS Collaboration, ATLAS-CONF-2016-037.
- [54] E. Alvarez, D. A. Faroughy, J. F. Kamenik, R. Morales, and A. Szykman, *Nucl. Phys.* **B915**, 19 (2017).
- [55] A. M. Sirunyan *et al.* (CMS Collaboration), *Eur. Phys. J. C* **77**, 578 (2017).
- [56] M. L. Mangano, M. Moretti, F. Piccinini, and M. Treccani, *J. High Energy Phys.* **01** (2007) 013.
- [57] J. Alwall *et al.*, *Eur. Phys. J. C* **53**, 473 (2008).
- [58] J. Campbell, R. K. Ellis, and R. Röntsch, *Phys. Rev. D* **87**, 114006 (2013).
- [59] J. M. Campbell and R. K. Ellis, *J. High Energy Phys.* **07** (2012) 052.
- [60] SM Higgs production cross sections at  $\sqrt{s} = 14$  TeV: <https://twiki.cern.ch/twiki/bin/view/LHCPhysics/CERNYellowReportPageAt14TeV2010>.
- [61] ATLAS-CMS recommended  $t\bar{t}$  cross section predictions: <https://twiki.cern.ch/twiki/bin/view/LHCPhysics/TtbarNNLO>.
- [62] Y. Li and F. Petriello, *Phys. Rev. D* **86**, 094034 (2012).
- [63] G. Cowan, K. Cranmer, E. Gross, and O. Vitells, *Eur. Phys. J. C* **71**, 1554 (2011).
- [64] For a recent reference, see M. Carena and Z. Liu, *J. High Energy Phys.* **11** (2016) 159, and references therein.
- [65] M. Aaboud *et al.* (ATLAS Collaboration), *Phys. Rev. Lett.* **119**, 191803 (2017).
- [66] The ATLAS Collaboration, ATLAS-CONF-2020-039.
- [67] A. M. Sirunyan *et al.* (CMS Collaboration), *J. High Energy Phys.* **07** (2020) 126.
- [68] Y. Omura, E. Senaha, and K. Tobe, *Phys. Rev. D* **94**, 055019 (2016).
- [69] W.-S. Hou and G. Kumar, *Phys. Rev. D* **102**, 115017 (2020).
- [70] M. Buza, Y. Matiounine, J. Smith, and W. L. van Neerven, *Eur. Phys. J. C* **1**, 301 (1998).
- [71] F. Maltoni, G. Ridolfi, and M. Ubiali, *J. High Energy Phys.* **07** (2012) 022.
- [72] J. Butterworth *et al.*, *J. Phys. G* **43**, 023001 (2016).
- [73] W.-S. Hou, M. Kohda, T. Modak, and G.-G. Wong, *Phys. Lett. B* **800**, 135105 (2020).
- [74] E. Kou, P. Urquijo *et al.* (Belle II Collaboration), *Prog. Theor. Exp. Phys.* **2019**, 123C01 (2019).
- [75] See, for example, N. Craig, F. D'Eramo, P. Draper, S. Thomas, and H. Zhang, *J. High Energy Phys.* **06** (2015) 137; S. Kanemura, H. Yokoya, and Y.-J. Zheng, *Nucl. Phys.* **B898**, 286 (2015); S. Gori, I. W. Kim, N. R. Shah, and K. M. Zurek, *Phys. Rev. D* **93**, 075038 (2016); and Ref. [76]. These studies were done in 2HDM with  $Z_2$  symmetry.
- [76] N. Craig, J. Hajer, Y.-Y. Li, T. Liu, and H. Zhang, *J. High Energy Phys.* **01** (2017) 018.